Orbitally relieved magnetic frustration in $NaVO_2$

Ting Jia, Guoren Zhang, and Zhi Zeng*
Key Laboratory of Materials Physics, Institute of Solid State Physics, Chinese Academy of Sciences, Hefei 230031, People's Republic of China

H. Q. Lin
Department of Physics and Institute of Theoretical Physics, The Chinese University of Hong Kong, Shatin, Hong Kong, People's Republic of China

(Received 26 February 2009; revised manuscript received 15 June 2009; published 6 July 2009)

The magnetic properties of $NaVO_2$ are investigated using full-potential linearized augmented plane-wave method. We perform calculations for three structures. For the rhombohedral structure at 100 K, the t_{2g} orbitals of V ions are split into upper a_{1g} and lower e_g' orbitals by a trigonal distortion of compression. For the monoclinic structure at 91.5 K, the system behaves such as a frustrated spin lattice with spatially anisotropic exchange interactions. For another monoclinic structure at 20 K, the magnetic frustration is relieved by a lattice distortion which is driven by a certain orbital ordering and the long-range magnetic ordering is thus formed. Moreover, the small magnetic moment originates from the compensation of orbital moment for the spin moment.

DOI: 10.1103/PhysRevB.80.045103 PACS number(s): 71.27.+a, 75.50.Ee, 75.30.Kz, 75.25.+z

I. INTRODUCTION

The compounds with a common chemical formula ATO_2 (A=Na or Li, T=3d transition metals) have been attracting a lot of attention for their large variety and richness in physical phenomena.[1–6] Indeed, the discovery of superconductivity in the $Na_{0.35}CoO_2 \cdot 1.3H_2O$ (Ref. 1) and the application of $LiCoO_2$ in rechargeable Li batteries have accelerated investigations on their fundamental physics. In addition, $NaMnO_2$ undergoes a structural phase transition at 45 K to a long-range ordered antiferromagnetic (AFM) ground state,[2] while $NaNiO_2$ exhibits ferromagnetic (FM) coupling in Ni-Ni plane below transition temperature.[3] Furthermore, a well-known member of this group, $LiNiO_2$, has no long-range magnetic ordering even at low temperatures.[4,7–9] The orbital frustration has been used to explain the absence of magnetic ordering,[4,7,8] and a local ordering of Ni^{3+} Jahn-Teller orbitals is also proposed to be responsible for the complex magnetic properties.[9] Therefore, its controversial magnetic properties have been attracting considerable interest.

These various phenomena always relate to the quasi-two-dimensional (2D) triangular lattice formed by T cations. Such a triangular lattice may lead to magnetic frustration, since all nearest-neighbor AFM interactions cannot be satisfied simultaneously.[2,5,6] Nevertheless, the magnetic frustration can be relieved by a certain orbital ordering (OO),[10–12] such as in $LiVO_2$ (Ref. 13) and $NaVO_2$.[14] $LiVO_2$ has been found to form a spin-singlet phase with corresponding OO at low temperatures,[5,13] whereas, its sister compound $NaVO_2$ displays very different behaviors.

Recently, Onoda *et al.*[15] have revealed a superparamagnetic state driven by the short-range ordered spin-one (the total spin in one trimer S=1) trimerization[16] below the transition temperature (T=98 K). However, McQueen *et al.*[14] have reported two successive OO transitions in $NaVO_2$. At 98 K, the system undergoes a continuous phase transition from a rhombohedral (R-3m) phase to a monoclinic ($C2/m$) one, corresponding to the proposed OO of one electron per V^{3+}. Below 93 K, the system undergoes a discontinuous phase transition to another monoclinic ($C2/m$) phase, consistent with the proposed OO of two electron per V^{3+}. In addition, a long-range ordered AFM state is formed at low temperatures, while the magnetic moment observed in the ordered phase is about 0.98 μ_B, much smaller than the expected value (2 μ_B). The controversial magnetic states below 98 K obtained by these two groups bring us interests and the puzzling magnetic moment deserves to be explored. To the best of our knowledge, there are possibly no theoretical reports yet, therefore we expect to understand its magnetic properties at low temperatures upon our theoretical efforts.

In the present work, we have performed first-principles calculations to investigate the electronic structures of $NaVO_2$, further to reveal the most possible orbital and magnetic orderings, and to explore the origin of small magnetic moment observed at low temperatures. Partially in agreement with the experimental findings,[14] the OO, accompanied by a long-range magnetic ordering, is found for the second monoclinic structure. And the observed magnetic moment can be explained by including the spin-orbit coupling (SOC) interactions.

This paper is organized as follows. The crystal structure and computational details are described briefly in Sec. II and the results and discussions are presented in Sec. III. Finally, a brief conclusion is summarized in Sec. IV.

II. CRYSTAL STRUCTURE AND COMPUTATIONAL DETAILS

The lattice parameters provided by McQueen *et al.* are listed in Table I. The structure of $NaVO_2$ is composed of two-dimensional (2D) triangular lattice VO_2 layers of edge sharing VO_6 octahedra separated by sodium ions, which is rhombohedral (R-3m) at relatively high temperature (HT) (T>98 K) and monoclinic ($C2/m$) in both intermediate temperature (IT) (91.5 K<T<98 K) and low-temperature

TABLE I. The lattice parameters of $NaVO_2$ at 100, 91.5, and 20 K.

Temperature	100 K	91.5 K	20 K
Space group	*R*-3*m*	*C*2/*m*	*C*2/*m*
a (Å)	2.9959(1)	5.1758(1)	5.2223(2)
b (Å)	2.9959(1)	3.0078(1)	2.9755(1)
c (Å)	16.0996(1)	5.6340(1)	5.6492(3)
α (deg)	90	90	90
β (deg)	90	107.629(1)	108.335(1)
γ (deg)	120	90	90
x,*y*,*z*(Na)	3*a*(0,0,0)	2*a*(0,0,0)	2*a*(0,0,0)
x,*y*,*z*(V)	3*b*(0,0,0.5)	2*d*(0,0.5,0.5)	2*d*(0,0.5,0.5)
x,*y*,*z*(O)	6*c*[0,0,0.2339(0)]	4*i*[0.2368(7),0,0.6989(5)]	4*i*[0.2296(5),0,0.7005(4)]

(LT) ($T<91.5$ K) phases.[14] At 100 K, the V-O distances are nearly 2.04 Å, but the O-V-O angle α is only 85.53° (Fig. 1). With lowering the temperature, α further reduces to 85.42° at 91.5 K and 85.13° at 20 K. Therefore, even in the HT phase, VO_6 octahedra in $NaVO_2$ have been different from the regular ones under a trigonal distortion of compression along the threefold (111) axis,[14] which induces the lowering of the O_h local symmetry to D_{3d}. In VO_2 layers, the V-V geometry is built by two long (3.00781 Å) and four short (2.99316 Å) bonds in the IT phase, and reversely is built by two short (2.97551 Å) and four long (3.00526 Å) ones in the LT phase.[17] The interlayer V-V distance is about 5.6 Å.

All the calculations were performed using the standard full-potential linearized augmented plane-wave code WIEN2K.[18] The muffin-tin sphere radii of 2.22, 2.00, and 1.77 a.u. were chosen for the Na, V, and O atoms, respectively. The cut-off parameter $R_{mt}K_{\max}$ was chosen to be 7.0 and 100.

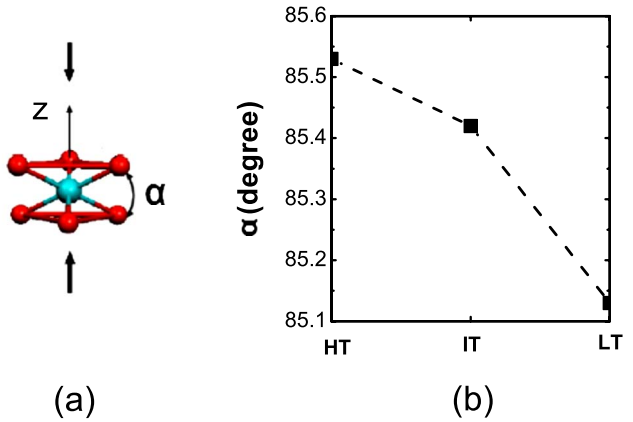

FIG. 1. (Color online) (a) The compressed octahedron of VO_2 layers. The *z* axis is the threefold axis of the VO_6 octahedron. α represents the O-V-O angle. (b) α angles in the HT, IT, and LT phases.

k points were used over the first Brillouin zone. The local spin-density approximation (LSDA) of Perdew and Wang[19] was used for the exchange and correlation potential. In order to take the strongly correlated nature of 3*d* electrons into account explicitly, we performed LSDA+*U* calculations,[20] where $U_{eff}=U-J$ (*U* and *J* are on-site Coulomb and exchange interaction, respectively) was used instead of *U*,[21] and the orbital-dependent potential has the form of $\Delta V_{FLL}=-U_{eff}(\hat{n}^{\sigma}-\frac{1}{2}I)$,[22] where $\hat{n}^{\sigma}$ is the orbital occupation matrix of spin σ. This type of double-counting correction has been called the fully localized limit.[23,24] For $NaVO_2$, we used $U_{eff}=3.6$ eV which has been used in its sister compound $LiVO_2$.[5] Note also that the conclusion made in this paper is not affected for $U_{eff}=2-6$ eV.[25] To explore the origin of small magnetic moment observed in the LT phase, we performed LSDA+SOC+*U* calculations, where the SOC is included by the second variational method with scalar relativistic wave functions.[18] The easy magnetization direction was set along the $(\bar{1}10)$ direction (short V-V bonds in the LT phase) observed in the experiment.[14]

In order to investigate different magnetic patterns, $2\times2\times2$ supercell was used in our calculations. We took into account two AFM structures in V-V plane as described in Fig. 2(a): I-type antiferromagnetism [Fig. 2(a)(i)] is AFM exchange along the (010) and $(\bar{1}10)$ directions with FM exchange along the (100) direction, (ii) II-type antiferromagnetism [Fig. 2(a)(ii)] is AFM exchange along the (100) and (010) directions with FM exchange along the $(\bar{1}10)$ direction. Totally there were five possible magnetic configurations in our calculations for the IT and LT phases [Fig. 2(b)]: ferromagnetic, *C*-AFI (I-type antiferromagnetism in plane, FM stacking), *C*-AFII (II-type antiferromagnetism in plane, FM stacking), *G*-AFI (I-type antiferromagnetism in plane, AFM stacking), and *G*-AFII (II-type antiferromagnetism in plane, AFM stacking).

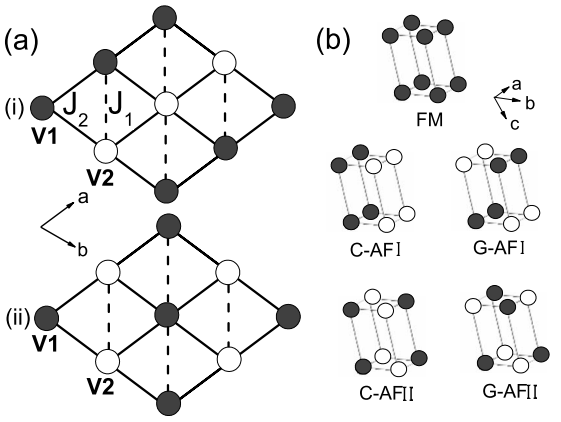

FIG. 2. (a) Two different magnetic patterns in V-V plane (i) I-type AF and (ii) II-type AF. The solid (dashed) lines represent short V-V bonds in the IT (LT) phase and dashed (solid) lines represent long V-V bonds in the IT (LT) phase. J_1 (J_2) denotes exchange interaction along the direction of dashed (solid) lines. (b) Schematic representation of five magnetic configurations used in our calculation. Only V atoms are drawn. Filled (open) circles indicate spin-up (down) moments.

III. RESULTS AND DISCUSSIONS

A. HT phase

As the paramagnetic behavior of $NaVO_2$ has been determined from the magnetic susceptibility measurements in the HT phase,[14,15] we just focus on the electronic structure instead of its magnetic properties.

The band structures obtained from LSDA and LSDA+U calculations are shown in Fig. 3. Within LSDA [Fig. 3(a)], the bands near the Fermi level (E_F) are mainly derived from V 3d states. Since straight V-O-V paths are not present in layered $NaVO_2$ and instead only nearly 90° V-O-V bonds exit, the V 3d states are quite narrow. In the approximately octahedral crystal field, the 3d orbitals are split into upper e_g and lower t_{2g} states. As shown in Fig. 3(a), e_g-derived bands range from 1.5 to 2.5 eV and t_{2g}-derived bands lie between −1.5 and 0.5 eV. The splitting between t_{2g} and e_g bands is about 1 eV. Under the trigonal crystal field, the t_{2g} orbitals are further split into one a_{1g} and two degenerate e_g' orbitals. However, the splitting is much less than the bandwidths so

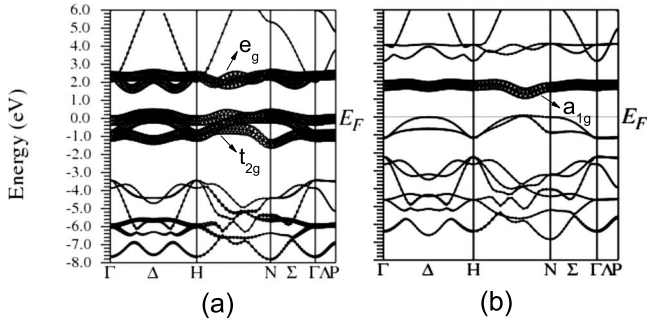

FIG. 3. The spin-majority band structure of $NaVO_2$ from (a) LSDA and (b) LSDA+U (U_{eff}=3.6 eV) calculations for the fixed structure at 100 K. The band with (a) 3d and (b) a_{1g} characters is marked.

that the t_{2g} orbitals still cross the E_F, which denotes a metallic state within LSDA. That is to say, LSDA calculations cannot reproduce the insulating nature of $NaVO_2$ from experiment.[14] The LSDA+U scheme[20] is thus used to count the strong correlation of V 3d electrons. As shown in Fig. 3(b), the empty a_{1g} band is pushed upwards by about 1 eV, and a gap is opened near the E_F. The system is hence an insulator due to electron correlation and $NaVO_2$ is indeed a good candidate for Mott-Hubbard insulator.

According to the pure crystal-field theory, the a_{1g} orbital is of lower energy than the e_g' orbitals under the trigonal distortion of compression, which is opposite to our LSDA+U results. So it is necessary to discuss the controversy on relative order of a_{1g}-e_g' in such trigonal distortions. In Ref. 26, Landron and Lepetit pointed out that this relative order is strongly influenced by the e_g-e_g' hybridization. The e_g and e_g' orbitals belong to the same irreducible representation (E_g) and can thus mix despite the large t_{2g}-e_g energy difference. Such a mix may be small but it modulates large energetic factors: the on-site Coulomb repulsions. When the e_g-e_g' hybridization is taken into account, the energy difference ΔE between the a_{1g} and e_g' orbitals depends on two competitive parts: $\Delta E=\Delta E_1+\Delta E_2=\varepsilon(a_{1g})-\varepsilon(e_g')$. ΔE_1 includes the kinetic energy, the electron charge interaction, and the interaction with the core electrons. ΔE_2 denotes the repulsion and exchange terms within the 3d shells. Additionally, ΔE_1 and ΔE_2 both depend on the amplitude of the trigonal distortion and are of opposite effect with each other. Under a trigonal distortion of compression, if we only consider the crystal-field effect (ΔE_1), the a_{1g} orbital is of lower energy than the e_g' orbitals ($\Delta E<0$). Whereas if we take ΔE_2 into account, the relative order between the a_{1g} and e_g' orbital is reversed ($\Delta E>0$), comparing with the crystal-field prediction. Therefore, LSDA+U calculations predict that the a_{1g} orbital is of higher energy than the e_g' orbitals in $NaVO_2$. In fact, such a controversy has been presented in another compressed triangular system Na_xCoO_2.[27–29] From the crystal-field theory, Koshibae and Maekawa[27] proposed that the energy of a_{1g} orbital is lower than the e_g' orbitals. However, the LDA+U method[28,29] yielded an a_{1g} orbital of higher energy than the e_g' orbitals. Later, the experimental results[30] showed that the Fermi surface of the CoO_2 layers issues from the a_{1g} orbital, not at all from the e_g' orbitals, supporting the LDA+U results.

B. IT phase

The triangular lattice of $NaVO_2$ exhibits magnetic frustration and spatially anisotropic exchange interactions in the IT phase. As shown in Table II, the G-AFI configuration is the most stable state among the five magnetic structures both from LSDA and LSDA+U calculations. By a detailed analysis of the magnetic ground state G-AFI, see [Fig. 2(a)(i)], AFM chains are formed along the $(\bar{1}10)$ direction (long V-V bonds), while AFM exchange is also more favorable along the (010) direction (short V-V bonds). Considering that all the short V-V bonds are completely equivalent, both the (100) and (010) directions should be AFM exchange. Thus, $NaVO_2$ in the IT phase can be regarded as a system with

TABLE II. The total energy E [meV/(8 f.u.)], magnetic moment M (μ_B) per V^{3+} and band gap E_g (eV) in different magnetic states.

		Configuration	FM	*C*-AFI	*G*-AFI	*C*-AFII	*G*-AFII
LSDA	IT (T=91.5 K)	E	514	4	0	128	132
		M	1.63	±1.37	±1.37	±1.34	±1.34
	LT (T=20 K)	E	574	152	156	4	0
		M	1.51	±1.35	±1.35	±1.38	±1.38
LSDA+U	IT (T=91.5 K)	E	329	65	0	192	189
		M	1.71	±1.65	±1.65	±1.66	±1.66
		E_g	1.1	1.2	1.1	1.4	1.5
	LT (T=20 K)	E	395	286	288	0	0
		M	1.71	±1.66	±1.66	±1.65	±1.65
		E_g	1.2	1.4	1.4	1.1	1.1

frustration effects. In addition, spatially anisotropic exchange interactions may exist in such a triangular spin lattice,[2] i.e., J_1 along the direction of long V-V bonds and J_2 along the two directions of short V-V bonds [Fig. 2(a)(i)].

In order to describe the magnetic frustration and spatially anisotropic exchange interaction more clearly, we estimate the exchange interactions along one of the triangle directions (J_1) and the other two (J_2) [Fig. 2(a)(i)]. Since all the configurations exhibit insulator characteristics, the spin size of V is stable, and the difference of total energy between *C*-AFI and *G*-AFI (*C*-AFII and *G*-AFII) configurations (see Table II) is so small that the system exhibits a 2D characteristic, a nearest-neighbor Heisenberg-type Hamiltonian may be a good primary approximation for the in-layer magnetic energy. The corresponding 2D spin Hamiltonian can be written as

$$H = J_1 \sum_{(k,l)} \mathbf{S}_k \cdot \mathbf{S}_l + J_2 \sum_{(i,j)} \mathbf{S}_i \cdot \mathbf{S}_j \tag{1}$$

where (i,j) denotes a nearest-neighbor pair (short V-V bond) and (k,l) denotes a next-nearest-neighbor pair (long V-V bond). By mapping the obtained total energies for each magnetic state to the Heisenberg model, the exchange interactions J_1 and J_2 were calculated within this approximation

$$2 \times (8 \times 4J_2S^2) = E(\mathrm{FM}) - E(C - \mathrm{AFII}), \tag{2}$$

$$2 \times (4 \times 4J_2S^2 + 4 \times 4J_1S^2) = E(\mathrm{FM}) - E(C - \mathrm{AFI}), \tag{3}$$

with S=1, we get J_2=2.1 meV and J_1=6.1 meV for $NaVO_2$ in the IT phase, which reflects strong spatial anisotropy. The AFM chains are established along the $(\bar{1}10)$ direction (J_1) and the interchain coupling (J_2) is frustrated. Moreover, the value of J_2/J_1=0.3 is so small that this magnetic structure can be described as so-called weakly coupled *zigzag* (S=1) chains model.[31]

The integer spins (S=1) are able to weaken the frustration effects in the frustrated systems, as in kagomé lattice.[32] Such a lattice has four nearest neighbors with the adjacent triangles on the lattice sharing only one lattice point. Interestingly, the triangular lattice can be composed of four kagomé lattices.[27] Thus, there are some analogous properties in these two frustrated systems. Therefore, it is reasonable to suppose that the triangular lattice also has the rule that the half-odd-integer spins are more highly frustrated than integer ones. For example, $NaTiO_2$ ($S=\frac{1}{2}$) (Ref. 5) and $LiCrO_2$ ($S=\frac{3}{2}$) (Ref. 6) with half-odd-integer spins are always frustrated even at low T, while the magnetic frustration of $NaMnO_2$ (S=2) is clearly lifted by a structural distortion.[2] Besides $NaMnO_2$, $NaVO_2$ is another typical triangular lattice with integer spins (S=1). Therefore, we can presume that the magnetic frustration in $NaVO_2$ can be lifted in some ways.

C. LT phase

From the discussion above, we expect that $NaVO_2$ with S=1 will show a long-range magnetic ordering or a finite ground-state magnetization at low T. As shown in Table II, *G*-AFII is only 0.3 meV lower in total energy than *C*-AFII within LSDA, and both *G*-AFII and *C*-AFII have the same lowest total energy from LSDA+U results for the LT phase. This reflects the obvious 2D characteristic of $NaVO_2$: the interlayer interaction is much weaker than the intralayer one. As stacking antiferromagnetically between layers is observed in the experiment,[14] *G*-AFII state should be more favorable at low T. Such a magnetic state denotes the long-range three-dimensional magnetic ordering with AFM-coupled FM chains in V cation layers and interlayer AFM coupling. Obviously, the magnetic frustration is lifted in *G*-AFII state by the first-order transition at 91.5 K: the lattice distorts to another monoclinic ($C2/m$) with four long and two short V-V bonds reversed, comparing with the IT phase.

The lattice distortion, which relieves the frustration, is driven by the formation of OO in the LT phase. Figure 4 shows the orbital characteristic of V 3*d* in *G*-AFII state. Since the orbital occupancies of the two inequivalent V [V1 and V2 in Fig. 2(a)(ii)] are nearly the same, only the density of states (DOS) of V1 3*d* is shown. The z axis of local coordinate system coincides with the V-O bond of the VO_6 octahedra. In such a coordinate system, d_{zx} and d_{yz} orbitals are mainly occupied and d_{xy} orbital is less occupied at all V ions. Such an orbital occupancy is consistent with the OO

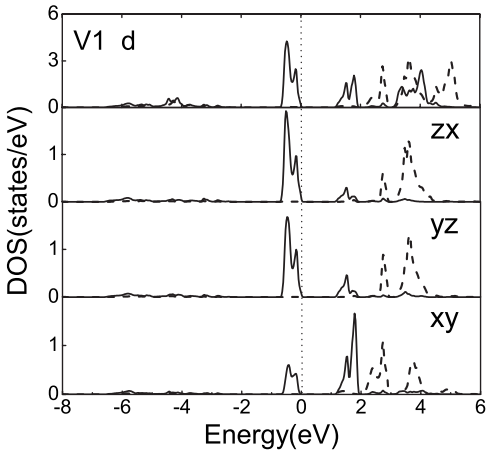

FIG. 4. DOS of $NaVO_2$ calculated by LSDA+U (U_{eff} =3.6 eV) in the G-AFII state for the fixed structure at 20 K. Besides total 3d state, all the d_{zx}, d_{yz}, and d_{xy} orbitals in local coordinate system for V1 [Fig. 2(a)(i)] ion are depicted. Solid (dashed) lines denote the spin-up (down) states.

proposed by McQueen and Cava:[14] the d_{zx} and d_{yz} orbitals are singly occupied with all unoccupied d_{xy} orbitals.

This OO relieves the magnetic frustration and stabilizes the long-range magnetic ordering state. In view of the weak superexchange interaction resulted from the nearly 90° angle of V-O-V (Ref. 33) as well as the weak magnetic interaction between adjacent VO_2 planes interleaved by a layer of Na ions, the V-V direct exchange interaction in plane should be dominant in such a particular crystal structure. Particularly, we only consider the σ overlap in V-V direct exchange, which is much stronger than the π overlap. It means that each orbital in a V ion only hybridizes with the same orbitals in the two nearest-neighboring V ions. That is to say, d_{yz} orbital hybridizes with two neighboring d_{yz} orbitals in the (010) and (0$\bar{1}$0) directions, and the d_{zx} orbital hybridizes with two neighboring d_{zx} orbitals in the (100) and ($\bar{1}$00) directions. The repulsions between the occupied orbitals (d_{zx} or d_{yz}) induce the elongation of V-V bonds along four directions: (010), (0$\bar{1}$0), (100), and ($\bar{1}$00). According to the Goodenough-Kanamori rules,[34] the strong AFM coupling should exist along these four directions because of the occupation of two orbitals with σ overlap. At the same time, the less occupancy of d_{xy} orbital leads to V-V bonds contraction as well as a weak FM exchange along the (1$\bar{1}$0) and ($\bar{1}$10) directions. Thus, the four long and two short V-V bonds result from bonding via d_{zx} and d_{yz} orbitals, with no bonding of the d_{xy} electrons. In other words, such an OO results in the lattice distortion, and consequently relieves the magnetic frustration.

In the LT phase, another important aspect is that the SOC turns out to be crucial for the small magnetic moment of 0.98 μ_B per V^{3+} observed experimentally.[14] As shown in Table II, the magnetic moments from LSDA+U calculations are much larger than the ones observed in the experiment. Further to investigate the magnetic moments changing with the particular choice of U_{eff}, we calculate the moments for U_{eff}=2–6 eV and find that the moments are not sensitive to

TABLE III. The band gap E_g (eV) and magnetic moment M (μ_B) per V^{3+} for different U_{eff} (eV) in G-AFII configuration.

U_{eff}	2	3	3.6	5	6
E_g	0.02	0.9	1.1	1.8	2.3
M	±1.57	±1.63	±1.65	±1.69	±1.71

U_{eff}, as shown in Table III, the magnetic moments stay constant within 0.2 μ_B as long as the system is an insulator. Since an easy magnetization direction ($\bar{1}$10) is observed in the experiment,[14] the SOC may play an important role in determining the total magnetic moment. Thus, the SOC is included to reinvestigate the magnetic moment.

Then, we perform LSDA+SOC+U calculations for the favorable magnetic configuration (G-AFII), and obtain a local moment of 0.89 μ_B per V^{3+} with 1.65 μ_B spin and −0.77 μ_B orbital contributions. This value is half the expected moment (2 μ_B), but very close to the observed one (0.98 μ_B). The DOS projected on ($2,m$) space shown in Fig. 5 reveals the origin of orbital moment. Note that the z axis is set to the direction of easy magnetization along ($\bar{1}$10) now. Since d_1 and d_{-1} have nearly the same occupancies, the orbital moment only comes from the contribution of different occupancies between d_2 and d_{-2}. By further analysis, the d_2 occupancy is less than one half of the d_{-2} one, which should give an orbital moment between 1 μ_B and 2 μ_B. Nevertheless, there is no surprise that the calculated orbital moment is 0.77 μ_B here, because some hybridization effects are neglected in the above analysis, e.g., the covalence effects with O 2p. Thus, the inclusion of SOC leads to a surprising but experimentally sound results.

IV. CONCLUSIONS

In summary, we have investigated the electronic structure and magnetic properties of $NaVO_2$ by first-principles calculations. The t_{2g} orbitals are split into upper a_{1g} and lower e_g'

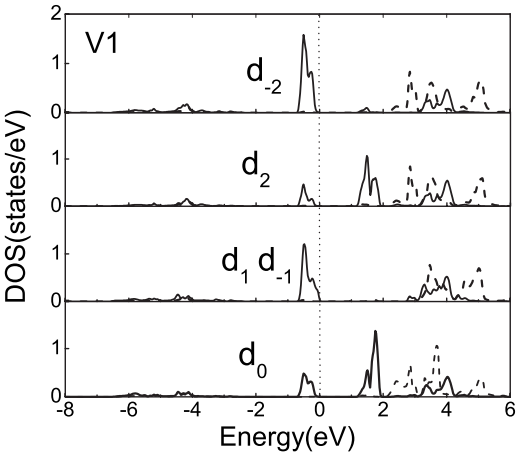

FIG. 5. DOS of $NaVO_2$ calculated by LSDA+U+SOC (U_{eff} =3.6 eV) in the G-AFII state for the fixed structure at 20 K. Solid (dashed) lines denote the spin-up (down) states.

states by a trigonal distortion of compression in the HT phase, which is similar to the splitting in Na_xCoO_2.[28] In the IT phase, the crystal symmetry is lowered to $C2/m$, under which the system behaves like a frustrated spin lattice with spatially anisotropic exchange interactions. Finally, a long-range ordered AFM ground state is formed when the magnetic frustration is relieved by another lattice distortion resulted from a certain ordering of occupied orbitals at low T. The small magnetic moment observed originates from the compensation of orbital moment for the spin moment. It is obvious that so many physical phenomena in the triangular lattice are reflected in $NaVO_2$, suggesting that $NaVO_2$ is a very good model material for studying 2D triangular lattice systems.

ACKNOWLEDGMENTS

We thank T. M. McQueen, P. W. Stephens, Q. Huang, T. Klimczuk, F. Ronning, and R. J. Cava for providing structural parameters prior to publication. This work was supported by the Special Funds for Major State Basic Research Project of China(973) of Ministry of Science and Technology of China under Grant No. 2007CB925004, 863 Project, Knowledge Innovation Program of Chinese Academy of Sciences, and Director Grants of CASHIPS, CUHK (Direct Grant No. 2060345). Part of the calculations were performed in Center for Computational Science of CASHIPS and the Shanghai Supercomputer Center.

*Corresponding author; zzeng@theory.issp.ac.cn

[1] K. Takada, H. Sakurai, E. Takayama-Muromachi, F. Izumi, R. A. Dilanian, and T. Sasali, Nature (London) **422**, 53 (2003).
[2] M. Giot, L. C. Chapon, J. Androulakis, M. A. Green, P. G. Radaelli, and A. Lappas, Phys. Rev. Lett. **99**, 247211 (2007).
[3] C. Darie, P. Bordet, S. de Brion, M. Holzapfel, O. Isnard, A. Lecchi, J. E. Lorenzo, and E. Suard, Eur. Phys. J. B **43**, 159 (2005).
[4] F. Reynaud, D. Mertz, F. Celestini, J.-M. Debierre, A. M. Ghorayeb, P. Simon, A. Stepanov, J. Voiron, and C. Delmas, Phys. Rev. Lett. **86**, 3638 (2001).
[5] S. Yu. Ezhov, V. I. Anisimov, H. F. Pen, D. I. Khomskii, and G. A. Sawatzky, Europhys. Lett. **44**, 491 (1998).
[6] I. I. Mazin, Phys. Rev. B **75**, 094407 (2007).
[7] A. J. W. Reitsma, L. F. Feiner, and A. M. Oleś, New J. Phys. **7**, 121 (2005).
[8] F. Mila, F. Vernay, A. Ralko, F. Becca, P. Fazekas, and K. Penc, J. Phys.: Condens. Matter **19**, 145201 (2007).
[9] J.-H. Chung, Th. Proffen, S. Shamoto, A. M. Ghorayeb, L. Croguennec, W. Tian, B. C. Sales, R. Jin, D. Mandrus, and T. Egami, Phys. Rev. B **71**, 064410 (2005).
[10] Y. Tokura and N. Nagaosa, Science, **288**, 462 (2000).
[11] J.-Q. Yan, J.-S. Zhou, and J. B. Goodenough, Phys. Rev. Lett. **93**, 235901 (2004).
[12] P. Horsch, A. M. Oleś, L. F. Feiner, and G. Khaliullin, Phys. Rev. Lett. **100**, 167205 (2008).
[13] H. F. Pen, J. van den Brink, D. I. Khomskii, and G. A. Sawatzky, Phys. Rev. Lett. **78**, 1323 (1997).
[14] T. M. McQueen, P. W. Stephens, Q. Huang, T. Klimczuk, F. Ronning, and R. J. Cava, Phys. Rev. Lett. **101**, 166402 (2008).
[15] M. Onoda, J. Phys.: Condens. Matter **20**, 145205 (2008).
[16] H. F. Pen, L. H. Tjeng, E. Pellegrin, F. M. F. de Groot, G. A. Sawatzky, M. A. van Veenendaal, and C. T. Chen, Phys. Rev. B **55**, 15500 (1997).
[17] The difference between 93 and 91.5 K has to do with the sample being measured on warming or on cooling. The IT to LT transition temperature is $T=91.5$ K here, corresponding to the lattice parameters measured on cooling and the slight lattice-parameter differences from Ref. 14 are within experimental error.
[18] P. Blaha *et al.*, http://www. wien2k
[19] J. P. Perdew and Y. Wang, Phys. Rev. B **45**, 13244 (1992).
[20] V. I. Anisimov, J. Zaanen, and O. K. Andersen, Phys. Rev. B **44**, 943 (1991).
[21] S. L. Dudarev, G. A. Botton, S. Y. Savrasov, C. J. Humphreys, and A. P. Sutton, Phys. Rev. B **57**, 1505 (1998).
[22] G. K. H. Madsen and P. Novak, Europhys. Lett. **69**, 777 (2005).
[23] V. I. Anisimov, I. V. Solovyev, M. A. Korotin, M. T. Czyżyk, and G. A. Sawatzky, Phys. Rev. B **48**, 16929 (1993).
[24] R. Laskowski, P. Blaha, and K. Schwarz, Phys. Rev. B **67**, 075102 (2003).
[25] We performed LSDA+U calculations for the two most stable configurations (G-AFI and G-AFII) both in the IT and LT phases with $U_{eff}=2,3,5,6$ eV. The results show that the G-AFI (G-AFII) is always the most stable state in the IT (LT) phase in such U_{eff} range.
[26] S. Landron and M.-B. Lepetit, Phys. Rev. B **77**, 125106 (2008).
[27] W. Koshibae and S. Maekawa, Phys. Rev. Lett. **91**, 257003 (2003).
[28] S. Landron and M.-B. Lepetit, Phys. Rev. B **74**, 184507 (2006).
[29] L.-J. Zou, J.-L. Wang, and Z. Zeng, Phys. Rev. B **69**, 132505 (2004).
[30] M. Z. Hasan, Y.-D. Chuang, D. Qian, Y. W. Li, Y. Kong, A. P. Kuprin, A. V. Fedorov, R. Kimmerling, E. Rotenberg, K. Rossnagel, Z. Hussain, H. Koh, N. S. Rogado, M. L. Foo, and R. J. Cava, Phys. Rev. Lett. **92**, 246402 (2004).
[31] Zheng Weihong, R. H. McKenzie, and R. P. Singh, Phys. Rev. B **59**, 14367 (1999).
[32] S. K. Pati and C. N. R. Rao, J. Chem. Phys. **123**, 234703 (2005).
[33] J. B. Goodenough, Phys. Rev. **117**, 1442 (1960).
[34] J. B. Goodenough, *Magnetism and the Chemical Bond* (Interscience, New York, 1963); J. Kanamori, J. Phys. Chem. Solids **10**, 87 (1959).